

# Learning Structured Communication for Multi-agent Reinforcement Learning

Junjie Sheng\*    Xiangfeng Wang†    Bo Jin‡    Junchi Yan§    Wenhao Li¶  
Tsung-Hui Chang||    Jun Wang\*\*    Hongyuan Zha††

February 12, 2020

## Abstract

This work explores the large-scale multi-agent communication mechanism under a multi-agent reinforcement learning (MARL) setting. We summarize the general categories of topology for communication structures in MARL literature, which are often manually specified. Then we propose a novel framework termed as Learning Structured Communication (**LSC**) by using a more flexible and efficient communication topology. Our framework allows for adaptive agent grouping to form different hierarchical formations over episodes, which is generated by an auxiliary task combined with a hierarchical routing protocol. Given each formed topology, a hierarchical graph neural network is learned to enable effective message information generation and propagation among inter- and intra-group communications. In contrast to existing communication mechanisms, our method has an explicit while learnable design for hierarchical communication. Experiments on challenging tasks show the proposed LSC enjoys high communication efficiency, scalability, and global cooperation capability.

## 1 Introduction

Reinforcement learning (RL) has achieved remarkable success in solving single-agent sequential decision problems under interactive and complicated environments, such as games [13, 18] and robotics [10]. In many real-world applications such as intelligent transportation systems [1] and unmanned systems [17], not only one, but usually a large number of agents are involved in the learning tasks. Such a setting naturally leads to the popular multi-agent reinforcement learning (MARL) problems, where the key research challenges include how to design scalable and efficient learning schemes under a non-stationary environment (caused by partial observation and/or the dynamics

---

\*School of Computer Science and Technology, East China Normal University, Shanghai 200092, China. (E-mail: 52194501003@stu.ecnu.edu.cn)

†School of Computer Science and Technology, East China Normal University, Shanghai 200062, China. (E-mail: xfwang@sei.ecnu.edu.cn)

‡School of Computer Science and Technology, East China Normal University, Shanghai 200062, China. (E-mail: bjin@cs.ecnu.edu.cn)

§Department of Computer Science and Engineering, Artificial Intelligence Institute, Shanghai Jiao Tong University, Shanghai 200240, China. (E-mail: yanjunchi@sjtu.edu.cn)

¶School of Computer Science and Technology, East China Normal University, Shanghai 200092, China. (E-mail: 52194501026@stu.ecnu.edu.cn)

||School of Science and Engineering, The Chinese University of Hong Kong (Shenzhen), Shenzhen, China. (Email: tsunghui.chang@ieee.org)

\*\*School of Computer Science and Technology, East China Normal University, Shanghai 200062, China. (E-mail: jwang@sei.ecnu.edu.cn)

††School of Computational Science and Engineering, College of Computing, Georgia Institute of Technology, USA. (E-mail: zha@cc.gatech.edu)

of other agents’ policies) with large and/or dynamic problem dimension, and complicated uncertain relationship between agents.

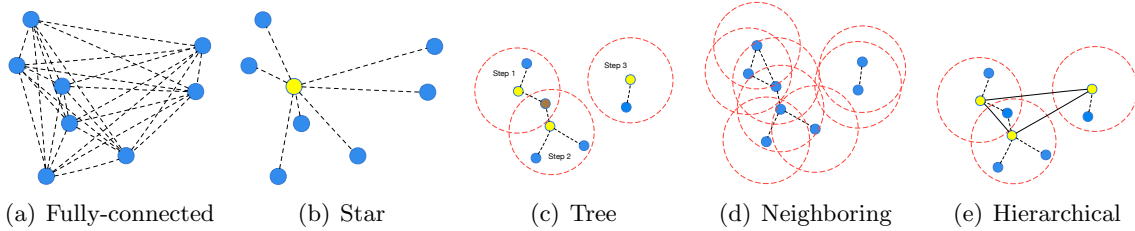


Figure 1: Topology of different communication structures, and LSC falls into the hierarchical one.

Learning to communicate effectively among agents has shown crucial to strengthen the inter-agent collaboration and ultimately improve the quality of policies learned by MARL. In this paper, we categorize the existing designs for communication topology<sup>1</sup> into four patterns: **i) Fully-connected:** DIAL [4], TarMAC [3] and SchedNet [9] use fully-connected communication structure (see Fig. 1(a)). Agents need to communicate with all the others, thus requiring high bandwidth when the number of agents is large. **ii) Star:** CommNet [4] and IC3 [19] assume star communication structure (see Fig. 1(b)). All agents need to transmit messages to the virtual central agent, incurring a major communication bottleneck. **iii) Tree:** ATOC [8] uses a tree communication structure. Agents only communicate with neighbors. However, communication must be allowed sequentially among groups, leading to high time complexity. **iv) neighboring:** DGN [7] uses neighboring communication structure. Agents communicate with neighbors concurrently to reduce communication costs.

We further analyze the above communication topology patterns by considering the accessibility and comprehension of messages for effective communication. Both the fully-connected structure and star structure ensure messages are accessible for all agents. While as discussed in ATOC [8], once a large number of messages emerge concurrently, extracting valuable information would become difficult. Tree structure and neighboring structure constrain the communication to neighbors and hence is able to improve message comprehension. To achieve global accessibility, they define neighbors as  $K$ -nearest agents and utilize multi-round communications. However, due to the lack of pooling mechanism, DGN [7] incurs two rounds of convolutions in communication; thus, only the information from two-hop distant agents is aggregated.

In this paper, we are aimed to improve both efficient message accessibility and effective message comprehension for large-scale MARL by proposing the so-called **Learning Structured Communication (LSC)** approach. Specifically, our LSC contains a structured communication module and a communication-based policy module. It aims to establish a hierarchical communication structure for learning the communication pattern as well as policy. In particular, a hierarchical communication structure (Fig. 1(e)) is established in a distributed fashion by a cluster-based routing protocol. To make the structure be formed dynamically for better cooperation, an auxiliary reinforcement task is designed to learn the communication weight in the end-to-end fashion. In the hierarchical structure, agents are grouped to different groups, and every group is assigned with a high-level agent. We design an intra-inter group communication mechanism to achieve global communication efficiently. Inter-group communication can help agents to capture global information better while intra-group communication helps fine-grained message exchanges. With these two modules, our experiments show that LSC can efficiently achieve global communication efficiency. The main highlights of this paper are summarized below.

1) We summarize the four existing categories of communication topology in the MARL literature, namely i) fully-connected, ii) star, iii) tree, and iv) neighboring, which are in general manually

<sup>1</sup>We interchangeably abuse the term topology and structure.

specified and fixed. We believe this perspective is enlightening for the design of new communication topology, given the fact that it has not been well organized in the existing literature.

2) We develop a new hierarchical communication topology LSC, which differs from the existing four patterns. Our approach allows for an adaptive formation of agents by dynamically grouping agents via a reinforcement learning procedure combined with a routing protocol. The messages can be jointly extracted and propagated through both intra- and inter-group communications via a hierarchical graph neural network.

3) Experimental results show that the proposed LSC yields promising results on public benchmarks in terms of communication efficiency, scalability, and global cooperation capability.

To our best knowledge, the current paper is the first work about hierarchical communication learning in MARL. We note that the idea of adopting hierarchical structure learning on MARL recently appears in HAMA [16]. The differences are obvious and fundamental: first, their hierarchy structure is used for learning agents' relation, but not for communication; second, their hierarchy design is fixed, other than adaptive and dynamically learned as done in this paper.

## 2 Related Work

**Learning-for-consensus.** These approaches try to let agents achieve consensus and cooperation directly from local observations, whereby a centralized training and decentralized execution framework (CTDE) is often used. Methods like MADDPG [11], QMIX [14], COMA [5] and MAAC [6] concatenate all the agents' observations and/or policies to obtain the state representation. This helps achieve better cooperation. However, the curse of dimensionality occurs when a large number of agents are present. HAMA [16] adopts a hierarchical graph attention network to leverage the group relationships. However, the groups are clustered by predefined rules, which is not feasible for complex scenarios.

**Learning-for-communication.** In these approaches, the agents aim to achieve consensus and cooperation through communications. Agents need to learn to communicate with others and process the received messages to enhance collaboration. As mentioned, the communication topology of the existing methods can be categorized as i) fully-connected (FC); ii) star; iii) tree; and iv) neighboring.

Fully-connected structures assume that each agent communicates with all the other agents. DIAL [4] learns what to communicate by back-propagating all the other agents' gradients to the message generation network. SchedNet [9] learns a weight-based scheduler to determine the communication priority based on DIAL, but the way of using the communication bandwidth is not scalable. Star structures assume agents only communicate with the single central agent as the hub. CommNet [4] aggregates all the agents' hidden states as the global message, thus can only be applied to cooperative scenarios. Extended from CommNet, IC3 [19] adds a communication gate to decide whether the agents to communicate. However, letting one agent handle all the messages in the star network cause a bottleneck at the central agent, both in communication bandwidth and information extraction. Tree and neighboring structures constrain communication to neighbors, thus avoids the single-point bottleneck issue. The  $K$ -nearest neighbor mechanism is often used to define neighbors. However, agents can distribute unevenly, and thereby choosing a good  $K$  is sometimes not easy in practical scenarios. ATOC [8] adopts tree structures, whereby each group in a chain (thus not hierarchical) performs communication sequentially. Although the inter-group communication can be achieved by the intersection of two groups, the large time complexity would be unbearable for real-time systems. To address the aforementioned difficulties, DGN [7] uses neighboring structured communication together with the graph convolution network (GCN). Multiple rounds of communications are adopted to enlarge the receptive field. As a common issue in GCN, shallow GCN without pooling layers can hardly explore rich global information as discussed in H-GCN [24]

**MARL with Graph Neural Network (GNN).** GNN is powerful in extracting relations among

entities, with emerging applications in MARL. RFM [21] designs an auxiliary action prediction task (predict other agents’ actions) with graph networks [2], which can help agents learn interpretable intermediate representations. MAGNet [12] uses heuristic rules to learn the relevant graph to help actor and critic learning. DGN [7] learns the GCN together with the relation kernel by minimizing the TD error, which can be applied to dynamic multi-agent RL problems. HAMA [16] adopts a hierarchical graph attention network based on a pre-defined hierarchical graph to help agents capture interrelations. The pre-defined and fixed group scheme used in HAMA limits its adaptability in dynamic scenarios.

In this paper, we target at learning both the underlying topology (with a hierarchy prior design) and the top-layered message extraction as well as the propagation process via GNNs. The message communication mechanism, the underlying topology as well as the way of using GNN in this paper all are novel and different from the existing works.

### 3 LSC: Learning Structured Communication

#### 3.1 Preliminaries and Overview

**Partial Observable Stochastic Games (POSG).** Agents learn policies by maximizing cumulative rewards via interacting with environment and other agents. POSG can be characterized as a tuple  $\langle \mathcal{I}, \mathcal{S}, b^0, \mathcal{A}, \mathcal{O}, \mathcal{P}, \mathcal{P}_e, \mathcal{R} \rangle$  where  $\mathcal{I}$  denotes the set of agents indexed from 1 to  $n$ ;  $\mathcal{S}$  is the finite set of states;  $b^0$  represents the initial state distribution and  $\mathcal{A}$  denotes the set of joint actions.  $A_i$  is the action space of agent  $i$ ,  $\mathbf{a} = \langle a_1, \dots, a_n \rangle$  denotes a joint action;  $\mathcal{O}$  denotes the joint observations and  $O_i$  is the observation space for agent  $i$ ,  $\mathbf{o} = \langle o_1, \dots, o_n \rangle$  denotes a joint observation;  $\mathcal{P}$  denotes the Markovian transition distribution with  $P(\tilde{s}, \mathbf{o} | s, \mathbf{a})$  being the probability of state  $s$  transiting to  $\tilde{s}$  with result  $\mathbf{o}$  after taking action  $\mathbf{a}$ .  $\mathcal{P}_e(\mathbf{o} | s)$  is the Markovian observation emission probability.  $\mathcal{R} : \mathcal{S} \times \mathcal{A} \rightarrow \mathbb{R}^n$  means the reward function.  $\mathbf{r} = \langle r_1, \dots, r_n \rangle$  denotes the joint reward each agent. The overall task of MARL can be solved by proper objective modeling, which may indicate, e.g., cooperative, competitive, or mixed relationship among agents.

**Deep Q-Learning.** Deep Q-Network (DQN) [13] is popular in deep RL as it is one of the few RL methods applicable to large-scale MARL. In each step, each agent observes state  $s$  and takes an action  $a$  based on policy  $\pi$ . It receives reward  $r$  and next state  $\tilde{s}$  from the environment. To maximize the cumulative reward after step  $t$ ,  $R_t = \sum_{k=t} r_k$ , DQN learns the action-value function  $Q^\pi(s, a) = \mathbb{E}_{s \sim \mathcal{P}, a \sim \pi(s)} [R_t | s_t = s, a_t = a]$  by minimizing  $\mathcal{L}(\theta) = \mathbb{E}_{s, a, r, \tilde{s}} [\tilde{y} - Q(s, a; \theta)]$ , where  $\tilde{y} = r + \gamma \max_{\tilde{a}} Q(\tilde{s}, \tilde{a}; \theta)$ . The agent follows  $\epsilon$ -greedy policy: select the action that maximizes the  $Q$ -value with probability  $1-\epsilon$  or randomly. Independent Deep Q-Learning (IDQN) [22] extends DQN by ignoring other agents for the POSG. Each agent learns a  $Q$ -function  $Q^a(u^a | s; \theta^a)$  based on its own observation and reward. Our LSC extends DQN with hierarchical communication.

**Proposed Approach Overview.** LSC takes the aforementioned formulation of POSG with the communication mechanism taken into account. Every agent needs to learn both action and communication policies. As discussed in MFRL [23], the Q-Learning family is more stable than on-policy methods in large-scale MARL. Hence, we choose DQN to learn the action policy with communication and form the global state perception.

To construct a hierarchical communication structure, LSC designs a flexible two-level communication topology, where agents are dynamically divided into high-level agents and low-level agents, indicated by the yellow and blue points in Fig.1(e). The high-level agents are in charge of forming global perception and coordinating low-level agents in their group. The low-level agents need to convey the local information to high-level agents. LSC includes two key modules: i) structured communication module and ii) communication-based policy module, as shown in Fig. 2. The first module aims to establish the dynamic hierarchical structured communication topology in a distributed fashion, while the second module contains the GNN-based communication extraction and  $Q$ -network

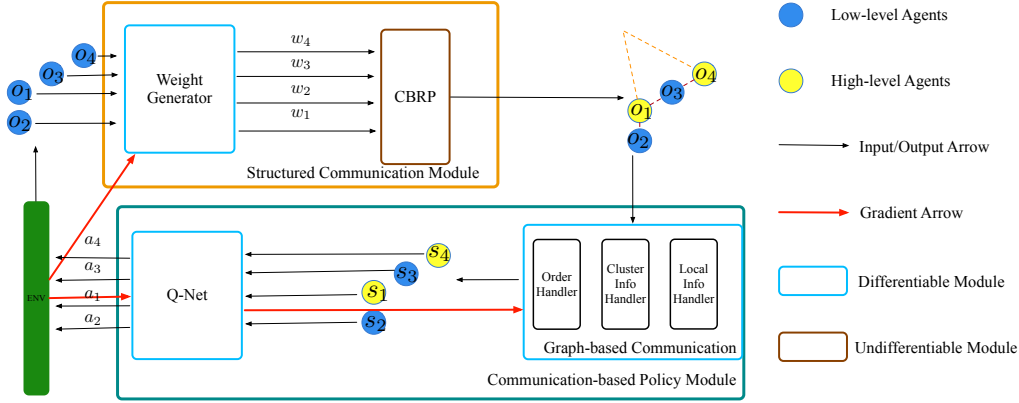


Figure 2: LSC with *Structured Communication Module* and *Communication-based Policy Module*, where  $s_i$ ,  $o_i$ ,  $a_i$  and  $w_i$  denote state (global perception), observation, action and importance weight of agent  $i$ , respectively. The former module uses partial observation to establish the communication structure. The latter employs Graph-based communication and Q-Network to extract communication content and produces collaboration policies respectively. based on established communication structure.

components.

### 3.2 Structured Communication Module

The structured communication module is designed by three principles: 1) agents in the same group are more likely to understand and cooperate inner group; 2) high-level agents are more likely to capture the global perception through the exchanged messages; 3) high-level agents are distributed sparsely to lower the communication cost. According to ATOC [8] and DGN [7], nearby agents are more likely to understand each other and form cooperation. Thus, we use the local geometrical relationship and the policy performance as our guide to establishing the hierarchical structure, as shown in Fig. 3.

Specifically, two sub-modules are included: the weight generator and the Cluster-Based Routing Protocol (CBRP). The weight generator sub-module aims to determine the importance of communication for each agent automatically. It is modeled by a neural network  $f_{wg} : o_i \rightarrow w_i$ , where the weight  $w_i$  can measure the confidence of an agent to become high-level. Further, the CBRP sub-module employs the weights of all agents  $\mathbf{w}$  and considers the local geometry to construct the hierarchical communication network. The CBRP sub-module can be implemented in a distributed fashion, leading to a distributed election of high-level agents. This advantage ensures the applicability of LSC to large-scale scenarios, which is demonstrated in the experiments.

The CBRP method [15] is a typical method for establishing a hierarchical routing structure. It takes a hyper-parameter cluster radius  $d$  as the basis to establish structure, and we denote the agent’s perceptive field as the area within cluster radius. Each low-level agent checks whether other agents have larger weights or contain high-level agents within its receptive area. If no such agent is found, this agent is elected as a high-level agent; otherwise, it keeps as a low-level agent. Meanwhile, each high-level agent checks whether other high-level agents exist in its receptive field. If no such agent is found or the founded high-level agents’ weights are smaller than its weights, it keeps as a high-level agent; otherwise, it downgrades to a low-level agent. After a sufficient number of rounds, the hierarchical structure would be established with sparsity: no high-level agent is included in other high-level agents’ receptive fields, which benefits communication efficiency. All agents are separated into groups with one high-level agent as the group leader. The overall hierarchical communication network is thus established: connecting high-level agents across groups, and connecting each low-level

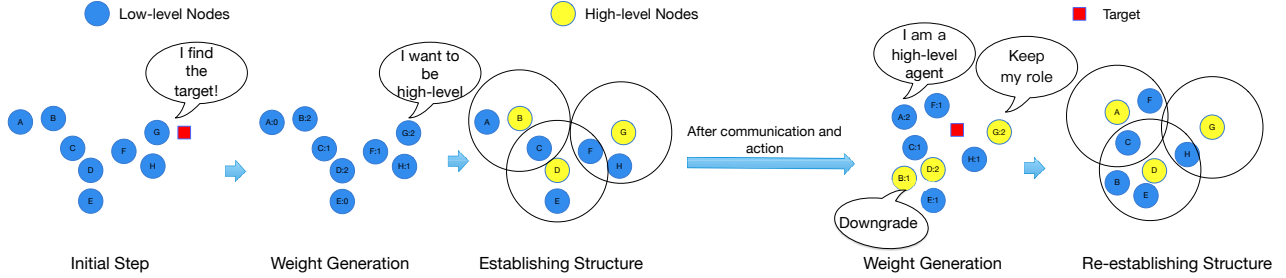


Figure 3: Procedure for dynamically establishing a hierarchical communication structure. Each agent determines its communication weight based on partial local observation. Agent ‘G’ finds the target (red square), then it has a higher weight 2 in the weight generation step. Then at the structure establishing step, it is elected as a high-level agent. After communication and actions, agents’ positions may change. Each agent needs to re-generate the communication weight and decide to keep or change their communication roles. For instance, ‘B’ gets a lower weight with a high weight agent ‘D’ nearby. Then ‘D’ will downgrade its role at the structure establishing step.

agent to its high-level agent.

A naive way of designing a weight generator is to set a fixed weight for all the agents simply. However, improper weights would result in a poor hierarchical structured communication network, which further causes the diverse performance of the communication-based policy. The experimental results also suggest that the choice of weights has a non-negligible influence on the performance, which motivates us to train these two modules end-to-end.

However, the CBRP sub-module is not differentiable, which means that the gradients cannot be back-propagated from the communication-based policy module to the weight generator sub-module. Therefore, we introduce an auxiliary RL task for weight generating, where the action for each agent is weight choosing with the same observation and reward of the original task, as well as practical constraints. Hence, we can have a close-loop task-driven communication weight generating manner. Specifically the weight  $w$  is defined in the discrete set  $\{0, 1, 2\}$ . IDQN is chosen to implement the weight generator for simplicity. The loss  $\ell(\theta^w)$  for the weight generator sub-module is:

$$\ell(\theta^w) = \mathbb{E}_{\mathbf{o}, \mathbf{w}, \mathbf{r}, \tilde{\mathbf{o}}} \left[ \sum_{i=1}^n (Q_{\theta^w}(o_i, w_i) - y_i)^2 \right]. \quad (3.1)$$

where  $y_i = r_i + \gamma \max_{\tilde{w}_i} Q_{\theta^w}(\tilde{o}_i, \tilde{w}_i)$ , and  $r_i$  denotes the reward for agent  $i$ .

### 3.3 Communication-based Policy Module

Once the communication network topology is determined, the communication-based policy module learns the communication message and generates a global collaboration policy. The communication-based policy module consists of two sub-modules: GNN-based communication sub-module and the Q-Net policy sub-module. The former is used to learn the communication messages and further update overall state perceptions. The latter learns the policy based on the new state perceptions after efficient communication.

As illustrated in Fig. 4, the well-established hierarchical structured communication network can be represented by a directed graph  $(\mathcal{V}, \mathcal{E})$ . The node set  $\mathcal{V}$  contains  $N_v$  nodes, which can be divided into the high-level node set  $\mathcal{V}_h$  and the low-level node set  $\mathcal{V}_l$ . For  $i \in \mathcal{V}_h$ , the node feature vector  $v_i$  includes the embedding feature  $v_i^n$ , the high-level node feature  $v_i^h$  and the global feature  $v_i^g$ ; for  $i \in \mathcal{V}_l$ , the node feature vector  $v_i$  only includes the embedding feature  $v_i^l$ . For each edge  $(i \rightarrow j) \in \mathcal{E}$  with

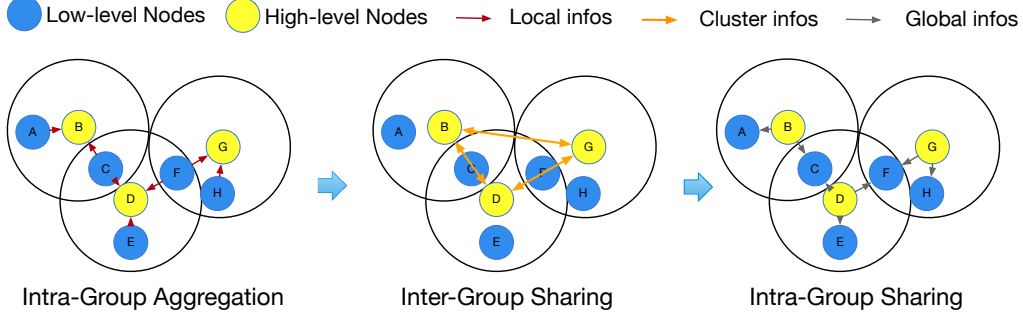


Figure 4: Intra-inter group communication. The edge embedding is considered as the communication message between agents. **Left:** Low-level agents transfer their valuable local embeddings to the associated high-level agents. **Middle:** High-level agents communicate with each other to form the global perception. **Right:** All high-level agents broadcast embedding information to their low-level agents to establish global cooperation.

Table 1: The proposed GNN-based communication architecture with three steps.

Type	Edge $(i \rightarrow j) \in \mathcal{E}$	Edge Update Scheme	Node Update Scheme
Step 1: intra-group aggregation	$i \in \mathcal{V}_l, j \in \mathcal{V}_h$	$e_{ij} = \phi(v_i^l), \bar{e}_j = \rho(\{e_{ij}\}_{(i \rightarrow j) \in \mathcal{E}})$	$v_j^h = \phi(\bar{e}_j, v_j^l)$
Step 2: inter-group sharing	$i \in \mathcal{V}_h, j \in \mathcal{V}_h$	$e_{ij} = \phi(v_i^h, v_i^l), \bar{e}_j = \rho(\{e_{ij}\}_{(i \rightarrow j) \in \mathcal{E}})$	$v_j^g = \phi(\bar{e}_j, v_j^l)$
Step 3: intra-group sharing	$i \in \mathcal{V}_h, j \in \mathcal{V}_l \cup \mathcal{V}_h$	$e_{ij} = \phi(v_i^g, v_i^h, v_i^l), \bar{e}_j = \rho(\{e_{ij}\}_{(i \rightarrow j) \in \mathcal{E}})$	$v_i^l = \phi(\bar{e}_i, v_i^l), v_j^l = \phi(\bar{e}_j, v_j^l)$

$i, j \in \mathcal{V}$ , the edge feature vector is denoted as  $e_{ij}$ . Functions  $\phi$  and  $\rho$  denote the update embedding function and aggregate function respectively. As shown in Fig. 4 and detailed in Table 1, the overall GNN-based communication sub-module consists of three steps.

**Step 1) Intra-group aggregation.** In each group, the low-level agents embed their local information and send it to the associated high-level agent  $j \in \mathcal{V}_h$ ; the high-level agents aggregate the information from all associated low-level agents and obtain the cluster perception;

**Step 2) Inter-group sharing.** The high-level agent communicates with the other high-level agent with cluster perception. This further aggregates all received other high-level messages to obtain the global perception;

**Step 3) Intra-group sharing.** Each of the high-level agents communicates all its features with the associated low-level agents while the low-level agents aggregate the received information from high-level agents. The embedding feature of both high-level and low-level agents are then updated.

The GNN-based communication sub-module is modeled as a GNN ( $f_{\theta^{gmn}}$ ) with parameter  $\theta^{gmn}$ , while the following  $Q$ -Net of agent  $i$  ( $Q_{\theta^Q}^i$ ) is parameterized by shared parameter  $\theta^Q$ . The gradient can be back-propagated from  $Q$ -Net to the graph neural network. As a result, the overall loss of communication-based policy module is as follows:

$$\ell(\theta^Q, \theta^{gmn}) = \mathbb{E}_{\mathbf{o}, \mathbf{a}, \mathbf{r}, \tilde{\mathbf{o}}} \left[ \sum_{i=1}^n (Q_{\theta^Q}^i(f_{\theta^{gmn}}(\mathbf{o}), a_i) - y_i)^2 \right], \quad (3.2)$$

where  $y_i = r_i + \gamma \max_{\tilde{a}_i} Q_{\theta^Q}^i(f_{\theta^{gmn}}(\tilde{\mathbf{o}}), \tilde{a}_i)$ , and  $r_i$  is the reward for agent  $i$ . Soft updating scheme is used:

$$\begin{aligned} \theta^{\bar{Q}} &= \tau \theta^Q + (1 - \tau) \theta^{\bar{Q}}, \\ \theta^{g\bar{mn}} &= \tau \theta^{gmn} + (1 - \tau) \theta^{g\bar{mn}}. \end{aligned} \quad (3.3)$$

The whole LSC is depicted in Algorithm 1. The CBRP function automatically and distributively establishes the structured communication network based on the learned importance weights.

---

**Algorithm 1 LSC: Learning Structured Communication**

---

```
1: Initialization: weight generator parameter:  $\theta^w$ ,  $Q$ -net:  $\theta^Q$ , GNN:  $\theta^{gnn}$ , target  $Q$ -net:  $\tilde{\theta}^Q$ , target  
   GNN:  $\tilde{\theta}^{gnn}$  replay buffer  $\mathcal{R} = \emptyset$ , cluster radius  $d$ , the number of agents  $n$ ;  
2: for Episode =  $1, \dots, M$  do  
3:   Reset  $t = 0$ , global state  $s^t$  and observation  $o_i^t$  for each agent  $i$ , low-level agents set  $\mathcal{V}_l^t =$   
   {all agents} and high-level agents set  $\mathcal{V}_h^t = \emptyset$ ;  
4:   for  $t = 1, \dots, T$  and  $s_t \neq$  terminal do  
5:     for each agent  $i$  do  
6:       With probability  $\epsilon$  pick a random action  $w_i^t$  else  $w_i^t = \arg \max_{\{w_i\}} Q_{\theta^w}(o_i^t)$ ;  
7:     end for  
8:     Get current position  $\text{POSS}_i^t$  of each agent  $i$ ;  
9:      $(\mathcal{V}_l^t, \mathcal{V}_h^t, \mathcal{E}) = \text{CBRP}((\mathcal{V}_l^{t-1}, \mathcal{V}_h^{t-1}), \{w_1^t, \dots, w_n^t\},$   
10:     $\{\text{POSS}_1^t, \dots, \text{POSS}_n^t\}, d)$ ;  
11:     $\{q_1^t, \dots, q_n^t\} = \text{HCOMM}(\mathcal{V}_l^t, \mathcal{V}_h^t, \mathcal{E})$ ;  
12:    for each agent  $i$  do  
13:      With probability  $\epsilon$  pick a random action  $a_i^t$  else choose action with the largest value  
    in  $q_i^t$ ;  
14:    end for  
15:    Execute global actions and get global reward  $r^t$ , next state  $s^{t+1}$ , next observation  $o^{t+1}$ ;  
16:    Get updated position  $\text{POSS}_i^{t+1}$  for each agent  $i$ ;  
17:    Store  $(s^t, o^t, \{\text{POSS}_1^t, \dots, \text{POSS}_n^t\}, a^t, r^t, o^{t+1},$   
18:     $\{\text{POSS}_1^{t+1}, \dots, \text{POSS}_n^{t+1}\}, s^{t+1})$  to  $\mathcal{R}$ ;  
19:    end for  
20:    for  $k = 1, \dots, K$  do  
21:      Sample a random mini-batch transitions from  $\mathcal{R}$ ;  
22:      Update weight generator  $\theta^w$  by Eq. (3.1);  
23:      Update communication based policy module  $(\theta^Q, \theta^{gnn})$  by minimizing Eq. (3.2);  
24:      Update the target networks through Eq. (3.3).  
25:    end for  
26: end for
```

Refer to Appendix for details of HCOMM and CBRP.

---

HCOMM denotes the communication-based policy module, which outputs the  $Q$ -values based on the GNN-based communication messages. The details of CBRP and HCOMM can be found in the Appendix.

### 3.4 Communication Efficiency Analysis

We discuss the communication efficiency<sup>2</sup> of our LSC from three aspects: the number of messages exchanged ( $N_{msg}$ ) among agents; the number of communication steps before acts ( $N_{step}$ ); the max communication bandwidth required for an agent ( $N_{b-r}$ ). Here the bandwidth is measured by the number of messages sent/received by the agent in each episode.

Table 2 compares the communication efficiency of different communication structures. In fully-connected (FC) structures where each agent communicates with all the others, the message exchanging complexity is  $\mathcal{O}(n^2)$ , and the max bandwidth for an agent is  $\mathcal{O}(n)$ . In the star structure, agents only need to communicate with the central agent, and thus the message exchanging complexity decrease to  $\mathcal{O}(n)$ . For the tree structure and neighboring structure, agents only need to communicate

---

<sup>2</sup>Communication efficiency varies by different communication mechanisms. Here our analysis is under the peer to peer mode.

Table 2: Structure comparison for communication efficiency.

	FC	Star	Tree	Neighbor	Hierarchical
$N_{msg}$	$\mathcal{O}(n^2)$	$\mathcal{O}(n)$	$\mathcal{O}(kb^2)$	$\mathcal{O}(kb^2)$	$\mathcal{O}(k^2 + kb)$
$N_{step}$	$\mathcal{O}(1)$	$\mathcal{O}(1)$	$\mathcal{O}(b)$	$\mathcal{O}(1)$	$\mathcal{O}(1)$
$N_{b-r}$	$\mathcal{O}(n)$	$\mathcal{O}(n)$	$\mathcal{O}(b)$	$\mathcal{O}(b)$	$\mathcal{O}(b + k)$

with neighbors. We denote the number of groups as  $k$  and the maximum number of agents in a group as  $b$ . The tree structure and neighboring structure need  $\mathcal{O}(kb^2)$  message exchanging complexity. The tree structure lets groups communicate sequentially, thus need  $\mathcal{O}(b)$  communication steps. Our hierarchical communication structure only needs low-level agents to communicate with the high-level agents, and high-level agents need to communicate with each other. Thus the message exchanging complexity is  $\mathcal{O}(kb + k^2)$ . Since  $k$  and  $b$  increase mildly with  $n$ , the proposed dynamic communication topology in LSC is suitable for large-scale MARL.

## 4 Experiments

We choose MAgent<sup>3</sup> and MPE<sup>4</sup> as our experiment platforms. Specifically, two scenarios are tested: i) battle and ii) cooperative spread. For compared baselines, first, we choose IDQN [22], which can be regarded as a degenerated version of our LSC with disabled communication. We also replace the adaptive hierarchical grouping component in our LSC with the star and neighboring topology for communication, as in CommNet [20] and DGN [7], respectively. We call these two variants LSC-star, LSC-nbor, and they serve as two benchmarks. They are all trained using Q-Learning, and the parameters are shared among agents. We refrain from directly comparing the proposed LSC with CommNet and DGN because they involve quite different techniques, and it is difficult to have a meaningful comparison. For a fair comparison, the basic hyperparameters of all methods under test are set the same. We adopt the graph\_nets[2] to implement the GNNs. The details of settings and hyperparameters are in the Appendix.

### 4.1 Task I: Large-scale Battle Game in MAgent

In this scenario (self-interested cooperative scenario),  $n$  agents move and fight against  $\ell$  enemies. The enemies have higher speed, higher attack power, and better stamina. Thus, agents need to form high-quality cooperation to wipe out enemies. The enemies are controlled by an IDQN [22] pretrained policy. To evaluate different methods, besides the learning curve, we choose some quantitative evaluation criteria of the battle game, like ‘Mean-reward’ (average per-step reward of all agents), ‘ $N_k$ ’ (average number of kills per episode), ‘ $N_d$ ’ (average number of deaths per episode) and ‘ $r_{kd}$ ’ (kill to death ratio  $N_k/N_d$ ).

We first compare the performance of different communication structures. All the models are trained with  $n = 64$  and  $\ell = 64$  for 1750 episodes. Fig. 5(a) shows the learning curve. The solid and shadow denote the mean and variance, respectively. As seen, LSC performs better in terms of the converged mean reward. We further test the learned models for 50 rounds, and the results are shown in Table 3. One can observe that LSC achieves a higher mean reward and a larger kill-death ratio. IDQN yields the lowest score due to a lack of communication schemes. Since LSC has additional intra-group communication when compared to LSC-nbor and extra inter-group communication between high-level agents when compared to LSC-star, the performance improvement of LSC over the two

<sup>3</sup><https://github.com/geek-ai/MAgent>

<sup>4</sup><https://github.com/openai/multiagent-particle-envs>

Table 3: Performance comparisons of 64 vs. 64 case in 50 testing trials on Battle game. The bold denotes the best result in each row.

Criteria / Method	LSC	LSC-star	LSC-nbor	IDQN
Mean-reward	<b>1.13</b>	1.04	0.94	0.89
$N_k$	<b>62.9</b>	61.36	62.4	59.3
$N_d$	<b>39.4</b>	48.52	43.6	55.8
$r_{kd}$	<b>1.60</b>	1.21	1.43	1.06

benchmarks well demonstrates the benefits brought by a hierarchical structure, intra-inter group communications.

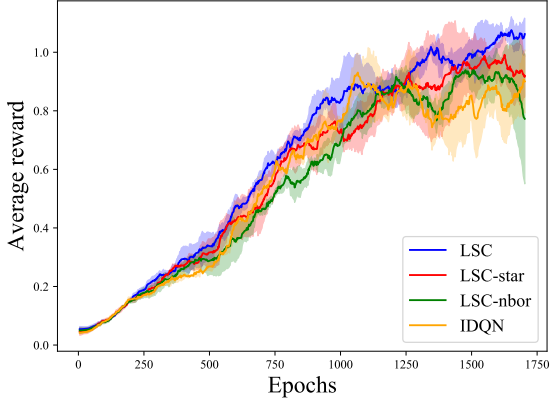
To investigate the impact of the learned importance weight generator, we compare LSC with a counterpart with a basic fixed weight generator (all agents are set to the same communication weight) in the battle scenario. In Fig. 5(b), our learned weight generator significantly outperforms the fixed one (LSC-fix). The result indicates that the structured communication module and communication-based policy module in LSC are strongly connected. We also compare LSC with LSC-star-gate (which incorporates communication gates in the star structure like IC3). In Fig. 5(c), one can see that LSC outperforms LSC-star-gate, and therefore the communication gate is barely beneficial.

Fig. 6 is presented to better understand the strategies learned by these algorithms. Specifically, LSC learns the encircle and fire focusing strategies as shown in Fig. 6(b) and Fig. 6(c). We find that the baselines can hardly handle the situation when some agents are far away from enemies. For example, the situation in Fig. 6(a), the agents in the top right can not know where to attack without communication. We let every learned model run from the initial state, and find only LSC learns to form an inter-group encircle and wipe out the enemies (see Fig. 6(d)). IDQN tends to cooperate within the visual range. Thus the agents that find no enemy would get close to the wall to defend attacks. Local cooperation leads to failed results, as shown in Fig. 6(e). Star and neighbor structures help agents form global cooperation. However, the agents far away from the majority have difficulty in comprehending the global information. In Fig. 6(f) and Fig. 6(g), such remote agents choose the spread out and exploration strategy, thus fail to wipe out enemies. To sum up, in Fig. 6(d), agents controlled by LSC form a global encircle strategy by communication in both intra-group and inter-group, which can wipe out enemies more efficiently.

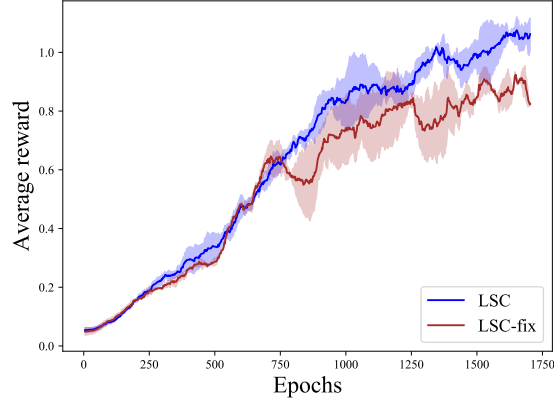
Fig.7 presents two weight-visualization graphs to show how the CBRP sub-module works. 7(a) visualizes the agent weights of an intermediate stage during the testing procedure for a  $64 \times 64$  battle. Red agents denote the enemies. As discussed in Section 3.2, only three kinds of discrete weights can be obtained for each agent, i.e.,  $\{0, 1, 2\}$ . The blue agents denote the agents have weight 2, and the green ones denote the agents have weight 1, while there is no agent with weight 0 in this stage. Without the CBRP sub-module, all the blue agents with weight 2 will be elected as high-level agents. This leads to an almost dense high-level agent structure, for instance, the red circle area. 7(b) visualize the agent weights after implementing CBRP method. Only three agents are set to be high-level agents (weight 2), while all others are set to be low-level agents (weight 0).

## 4.2 Task II: Cooperative Spread in MPE

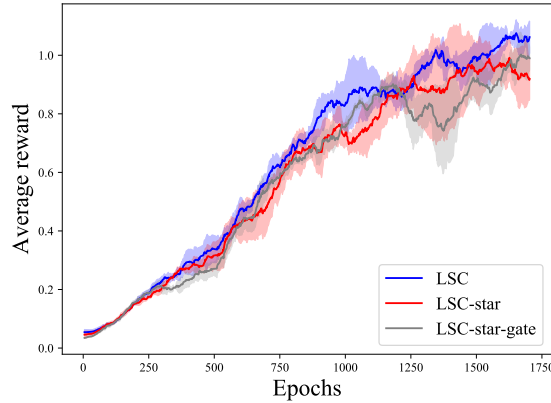
We design a new scenario: cooperative spread based on MPE [11], to test the performance of LSC in the fully cooperative scenario. There are 12 agents and 4 landmarks in this environment. Every landmark needs to be reached by three agents. However, when there are more than three agents reaching the landmark, the landmark would be overloaded and penalizes the agents. We train LSC and other baselines with 3000 episodes, whose learning curves are shown in Fig. 8. We take 50 test rounds on the obtained models, and Table 4 contains some evaluation criteria in the testing procedure, for instance ‘ $N_s$ ’ (number of successive reaching of three agents to one landmark), ‘ $N_o$ ’



(a) Structure comparison



(b) Weight generator comparison



(c) LSC and LSC-star-gate

Figure 5: Comparisons of learning curves in Battle game.

Table 4: Performance comparisons of 12 agents case in 50 testing trials). The bold stands for the best result in each row.

Method	LSC	LSC-star	LSC-nbor	IDQN
$N_s$	<b>156</b>	80	61	16
$N_o$	13	16	9	<b>2</b>
Mean-reward	<b>-54.6</b>	-68.2	-69.1	-78.1

(number of successive reaching of more than three agents to one landmark) and ‘Mean-reward’ (average per-episode reward of all agents).

Fig. 8 and Table 4 show LSC outperforms in training and testing. The high-level agents (in star or hierarchical topology) can help speed up the learning process by making an agreement of global information. Thus LSC and star topology learn faster than the other two. LSC converges to a higher reward than baselines. Table 4 shows IDQN’s strategy is passive. Agents avoid overload while taking less chance to reach the landmark. Star and neighboring structures take more aggressive strategies, and the star structure cannot achieve fine-grained information from neighbors, thus lead to more overloads. The neighboring structure makes some agents disconnected to others, thus cannot achieve global communication and lead to less chance for success. LSC achieves the highest reward during testing, with reasonable overload.

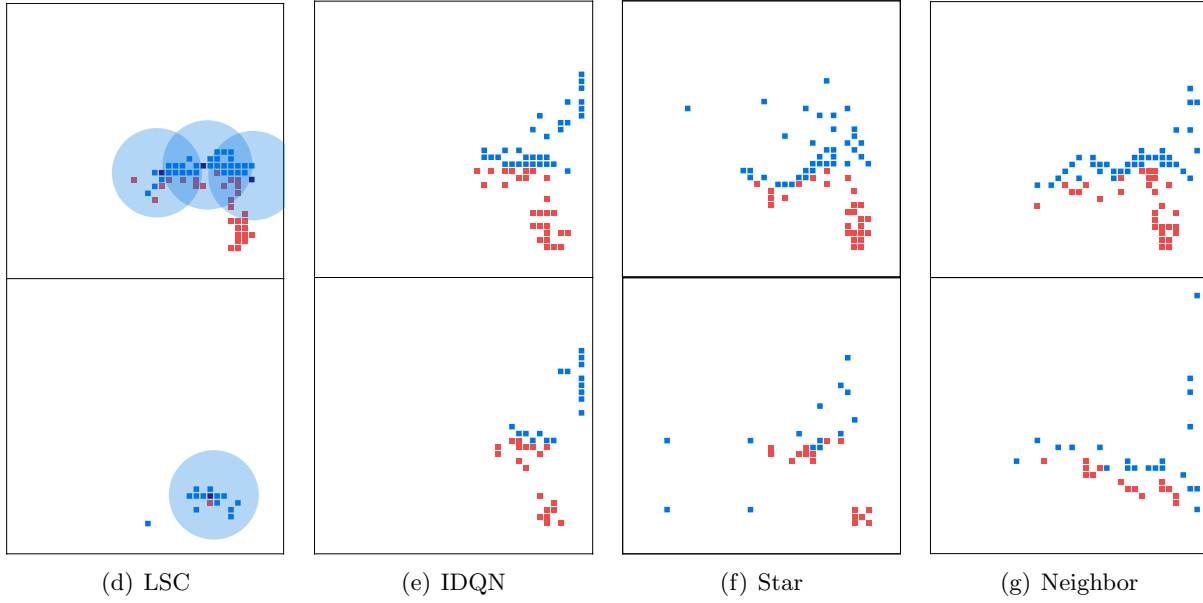
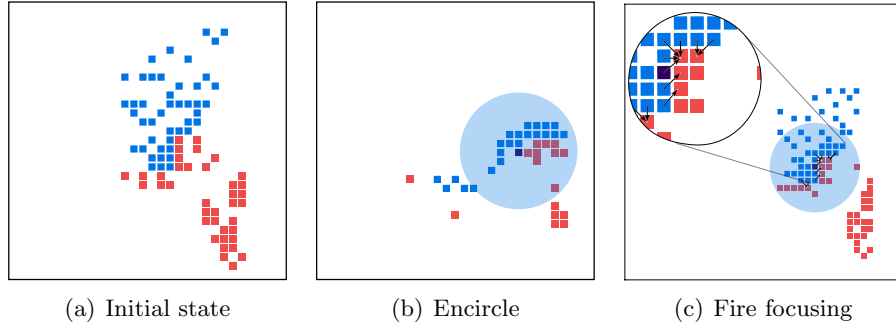


Figure 6: Behavior illustration. The first row shows two typical behavior by LSC. In the second row, the top and bottom plot denote the early state and the near to final battle state, respectively.

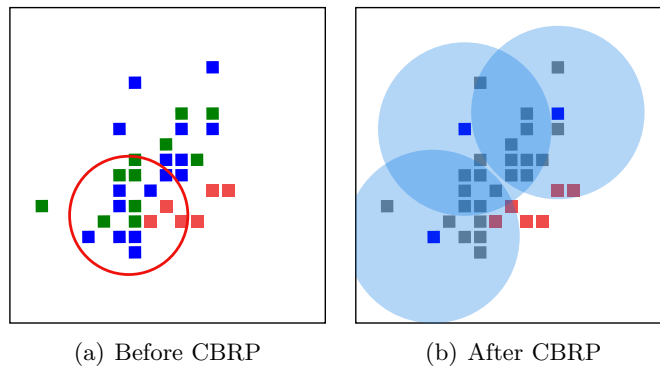


Figure 7: Weight visualization of dynamic communication structure: ‘Before CBRP’ and ‘After CBRP’ stages. Blue, green and grey nodes denote agents with weight 2, 1 and 0 (enemies in red).

## 5 Conclusion and Future Work

In this paper, a novel learning structured communication (LSC) algorithm has been proposed for multi-agent reinforcement learning. The hierarchical structure is self-learned with a clustering-based routing protocol. The communication message representation is then naturally embedded and ex-

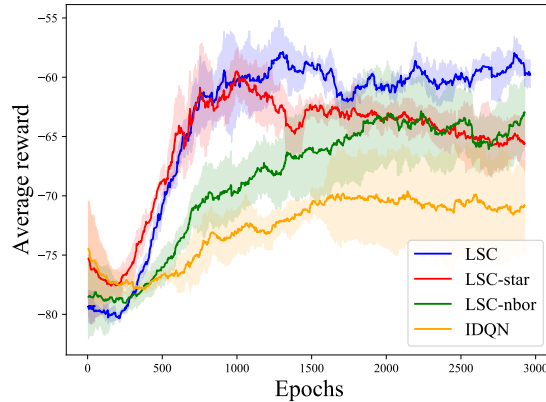


Figure 8: Learning curves on Cooperative Spread scenario in MPE.

tracted via a graph neural network. Experiments on two scenarios demonstrate that our LSC can outperform existing learning-to-communicate algorithms with better communication efficiency, cooperation capability, and scalability. In the future, it is worthwhile to improve LSC by considering some practical constraints such as communication bandwidth and latency.

## References

- [1] Jeffrey L Adler and Victor J Blue. A cooperative multi-agent transportation management and route guidance system. *Transportation Research Part C: Emerging Technologies*, 10(5-6):433–454, 2002.
- [2] Peter W Battaglia, Jessica B Hamrick, Victor Bapst, Alvaro Sanchez-Gonzalez, Vinicius Zambaldi, Mateusz Malinowski, Andrea Tacchetti, David Raposo, Adam Santoro, Ryan Faulkner, et al. Relational inductive biases, deep learning, and graph networks. *arXiv preprint arXiv:1806.01261*, 2018.
- [3] Abhishek Das, Théophile Gervet, Joshua Romoff, Dhruv Batra, Devi Parikh, Mike Rabbat, and Joelle Pineau. TarMAC: Targeted multi-agent communication. In *ICML*, pages 1538–1546, 2019.
- [4] Jakob Foerster, Ioannis Alexandros Assael, Nando de Freitas, and Shimon Whiteson. Learning to communicate with deep multi-agent reinforcement learning. In *NeurIPS*, pages 2137–2145, 2016.
- [5] Jakob N Foerster, Gregory Farquhar, Triantafyllos Afouras, Nantas Nardelli, and Shimon Whiteson. Counterfactual multi-agent policy gradients. In *AAAI*, pages 2974–2982, 2018.
- [6] Shariq Iqbal and Fei Sha. Actor-attention-critic for multi-agent reinforcement learning. In *ICML*, pages 2961–2970, 2019.
- [7] Jiechuan Jiang, Chen Dun, Tiejun Huang, and Zongqing Lu. Graph convolutional reinforcement learning. In *ICLR*, 2020.
- [8] Jiechuan Jiang and Zongqing Lu. Learning attentional communication for multi-agent cooperation. In *NeurIPS*, pages 7254–7264, 2018.
- [9] Daewoo Kim, Sangwoo Moon, David Hostallero, Wan Ju Kang, Taeyoung Lee, Kyunghwan Son, and Yung Yi. Learning to schedule communication in multi-agent reinforcement learning. In *ICLR*, 2019.
- [10] Timothy Lillicrap, Jonathan Hunt, Alexander Pritzel, Nicolas Heess, Tom Erez, Yuval Tassa, David Silver, and Daan Wierstra. Continuous control with deep reinforcement learning. In *ICLR*, 2016.
- [11] Ryan Lowe, Yi Wu, Aviv Tamar, Jean Harb, OpenAI Pieter Abbeel, and Igor Mordatch. Multi-agent actor-critic for mixed cooperative-competitive environments. In *NeurIPS*, pages 6379–6390, 2017.
- [12] Aleksandra Malysheva, Tegg Taekyong Sung, Chae-Bong Sohn, Daniel Kudenko, and Aleksei Shpilman. Deep multi-agent reinforcement learning with relevance graphs. *arXiv preprint arXiv:1811.12557*, 2018.

- [13] Volodymyr Mnih, Koray Kavukcuoglu, David Silver, Andrei A Rusu, Joel Veness, Marc G Bellemare, Alex Graves, Martin A Riedmiller, Andreas Fidjeland, Georg Ostrovski, Stig Petersen, Charles Beattie, Amir Sadik, Ioannis Antonoglou, Helen King, Dhharshan Kumaran, Daan Wierstra, Shane Legg, and Demis Hassabis. Human-level control through deep reinforcement learning. *Nature*, 518(7540):529–533, 2015.
- [14] Tabish Rashid, Mikayel Samvelyan, Christian Schroeder de Witt, Gregory Farquhar, Jakob Foerster, and Shimon Whiteson. QMIX: Monotonic value function factorisation for deep multi-agent reinforcement learning. In *ICML*, pages 4292–4301, 2018.
- [15] M Rezaee and M Yaghmaee. Cluster based routing protocol for mobile ad hoc networks. *INFOCOMP*, 8(1):30–36, 2009.
- [16] Heechang Ryu, Hayong Shin, and Jinkyoo Park. Multi-agent actor-critic with hierarchical graph attention network. *arXiv preprint arXiv:1909.12557*, 2019.
- [17] Elham Semsar-Kazerooni and Khashayar Khorasani. Multi-agent team cooperation: A game theory approach. *Automatica*, 45(10):2205–2213, 2009.
- [18] David Silver, Aja Huang, Chris J Maddison, Arthur Guez, Laurent Sifre, George van den Driessche, Julian Schrittwieser, Ioannis Antonoglou, Veda Panneershelvam, Marc Lanctot, Sander Dieleman, Dominik Grewe, John Nham, Nal Kalchbrenner, Ilya Sutskever, Timothy Lillicrap, Madeleine Leach, Koray Kavukcuoglu, Thore Graepel, and Demis Hassabis. Mastering the game of go with deep neural networks and tree search. *Nature*, 529(7587):484–489, January 2016.
- [19] Amanpreet Singh, Tushar Jain, and Sainbayar Sukhbaatar. Learning when to communicate at scale in multiagent cooperative and competitive tasks. In *ICLR*, 2019.
- [20] Sainbayar Sukhbaatar, Rob Fergus, et al. Learning multiagent communication with backpropagation. In *NeurIPS*, pages 2244–2252, 2016.
- [21] Andrea Tacchetti, H. Francis Song, Pedro A. M. Mediano, Vinicius Zambaldi, Jnos Kramr, Neil C. Rabinowitz, Thore Graepel, Matthew Botvinick, and Peter W. Battaglia. Relational forward models for multi-agent learning. In *ICLR*, 2019.
- [22] Ardi Tampuu, Tambet Matiisen, Dorian Kodelja, Ilya Kuzovkin, Kristjan Korjus, Juhan Aru, Jaan Aru, and Raul Vicente. Multiagent cooperation and competition with deep reinforcement learning. *PLOS ONE*, 12(4):1–15, 2017.
- [23] Yaodong Yang, Rui Luo, Minne Li, Ming Zhou, Weinan Zhang, and Jun Wang. Mean field multi-agent reinforcement learning. In *ICML*, pages 5571–5580, 2018.
- [24] Zhitao Ying, Jiaxuan You, Christopher Morris, Xiang Ren, Will Hamilton, and Jure Leskovec. Hierarchical graph representation learning with differentiable pooling. In *Advances in neural information processing systems*, pages 4800–4810, 2018.

# A Appendix

## A.1 Hyperparameters and Experimental settings

In MAgent battle, agents fight enemies in a  $40 \times 40$  grid world. Each agent in both sides has a  $6 \times 6$  perception field and can attack its 8-adjacent grids. The speed, attack power, and health point for each agent are 1, 1, and 4, which are increased to 2, 2, and 10 for the enemy to increase the difficulty. The reward is +5 for successful attacking an enemy, -2 for being killed, and -0.01 for attacking a blank grid.

In the cooperative spread, 12 agents need to cooperate to reach every landmark with three agents. Each agent can get the relative position of other agents while only when the landmark in its receptive field (distance smaller than 0.4) agent can get the landmark’s relative position. The action space contains UP, DOWN, LEFT, RIGHT, and STAY. When three agents reach a landmark (distance smaller than 0.2), the landmark will reward to all the agents with 2. However, if there are more than three agents reach a landmark, all the agents are penalized with -10. To help agents learn to reach landmarks, we add dense reward (landmarks give the negative-sum nearest three agents distance as a reward) like the typical spread setting.

To enable reproducibility, we summarize the hyperparameters for LSC and baselines at table 5. The weight generator’s hyper-parameters are all the same as IDQN, but the output layer sets to 3 (the level of weights).

Table 5: Hyperparamaters for LSC and baselines

Parameter	LSC	IDQN	LSC-star	LSC-nbor
discount( $\gamma$ )			0.98	
batch size			1/64	
$\epsilon_{start}$			1.0	
$\epsilon_{end}$			0.01	
optimizer			Adam	
learning rate			$1e^{-4}/1e^{-2}$	
Conv layers			2/—	
Aggregation			seg sum	
Q network			MLP(128,64)/MLP(64,64,5)	
Activation			ReLU	
dimension of msg	3	—	3	3
radius	6/0.6	—	6/0.6	6/0.6

## A.2 CBRP Function and HCOMM Function

We provide the CBRP and HCOMM function used in the LSC in Algorithm 2 and 3.

---

**Algorithm 2** CBRP: Cluster Based Routing Protocol

---

```
1: Input:  $(\mathcal{V}_l^t, \mathcal{V}_h^t), \{w_1^t, \dots, w_n^t\}, \{\mathbf{POSS}_1^t, \dots,$   
2:    $\mathbf{POSS}_n^t\}, d$   
3: Define neighbours are distance  $< d$ ,  $T_e$  is a constant to control the max-waiting time,  $\mathcal{V}_u = \emptyset$  is  
   the undecided nodes set and  $\mathcal{E} = \emptyset$ ;  
4: Each node  $i$  broadcast its weight  $w_i^t$  to neighbours;  
5: ‡ Maintain the structure  
6: for  $i$  is in high-level nodes set  $\mathcal{V}_h^t$  do  
7:   if there is a high-level nodes in neighbours and its weight is bigger than agent  $i$  then  
8:     Pop node  $i$  from  $\mathcal{V}_h^t$  and append it to  $\mathcal{V}_l^t$ ;  
9:   end if  
10: end for  
11: for  $i$  is in low-level nodes set  $\mathcal{V}_l^t$  and no high-level node is in its neighbour do  
12:   Pop node  $i$  from  $\mathcal{V}_l^t$  and append it to  $\mathcal{V}_u$ ;  
13: end for  
14: ‡ Elect high-level nodes  
15: for  $i$  is in  $\mathcal{V}_u$  concurrently do  
16:   if does not receive larger weight for  $T_e$  then  
17:     append  $i$  to  $\mathcal{V}_h^t$  and broadcast to neighbours;  
18:   else  
19:     Wait for the signal from high-level node for  $2T_e$ ;  
20:   end if  
21:   if received a signal from high-level node then  
22:     append  $i$  to  $\mathcal{V}_l^t$ ;  
23:   else  
24:     append  $i$  to  $\mathcal{V}_h^t$ ;  
25:   end if  
26: end for  
27: ‡ Generate communication link  
28: for  $i$  in  $\mathcal{V}_h^t$  do  
29:   for  $j$  in  $\mathcal{V}_i^t$  and  $j$  is neighbouring  $i$  do  
30:     append  $e_{ij} = 0$  and  $e_{ji} = 0$  to  $\mathcal{E}$ ;  
31:   end for  
32:   for  $j$  in  $\mathcal{V}_h^t$  do  
33:     append  $e_{ij} = 0$  to  $\mathcal{E}$ ;  
34:   end for  
35: end for  
36: Return  $(\mathcal{V}_l^t, \mathcal{V}_h^t, \mathcal{E})$ 
```

---

---

**Algorithm 3 HCOMM: Hierarchical Communication based Policy Module**


---

```

1: Input:  $\mathcal{V}_l, \mathcal{V}_h, \mathcal{E}$ ;
2: ‡ Intra-group aggregation
3: for  $v^i$  in  $\mathcal{V}_l$  do
4:   for  $v^j$  in  $\mathcal{V}_h$  and  $(i \rightarrow j)$  in  $\mathcal{E}$  do
5:      $e_{ij} = \phi^{enc}(v^i)$ ; ▷ Generate normal to central messages
6:   end for
7: end for
8: for  $v_j$  in  $\mathcal{V}_h$  do
9:    $\bar{e}_j = \rho(\{e_{ij}\}_{(i \rightarrow j) \in \mathcal{E}})$ ; ▷ Central agents aggregate received messages
10:   $v_j^h = \phi(\bar{e}_j, v_j^l)$ ; ▷ Generate cluster perception
11: end for
12: ‡ Inter-group sharing
13: for  $v_j$  in  $\mathcal{V}_h$  do
14:   for  $v_i$  in  $\mathcal{V}_h$  and  $(i \rightarrow j)$  in  $\mathcal{E}$  do
15:      $e_{ij} = \phi(v_i^h, v_i^l)$ ; ▷ Generate central to central messages
16:   end for
17: end for
18: for  $v_j$  in  $\mathcal{V}_h$  do
19:    $\bar{e}_j = \rho(\{e_{ij}\}_{(i \rightarrow j) \in \mathcal{E}})$ ; ▷ Aggregate received central to central messages
20:    $v_j^g = \phi(\bar{e}_j, v_j^l)$ ; ▷ Obtain global perception
21: end for
22: ‡ Intro-group sharing
23: for  $v_i$  in  $\mathcal{V}_h$  do
24:   for  $v_j$  in  $\mathcal{V}_l$  and  $(i \rightarrow j)$  in  $\mathcal{E}$  do
25:      $e_{ij} = \phi(v_i^g, v_i^h, v_i^l, e_{ji})$ ,  $\bar{e}_j = \rho(\{e_{ij}\}_{(i \rightarrow j) \in \mathcal{E}})$ ; ▷ Generate central to normal messages
26:   end for
27: end for
28: for  $v_j$  in  $\mathcal{V}_l \cup \mathcal{V}_h$  do
29:   for  $v_i$  in  $\mathcal{V}_h$  and  $(i \rightarrow j)$  in  $\mathcal{E}$  do
30:      $\bar{e}_j = \rho(\{e_{ij}\}_{(i \rightarrow j) \in \mathcal{E}})$ ; ▷ Aggregate received central to normal messages
31:   end for
32:    $v_j^n = \phi(\bar{e}_j, v_j^l)$ ; ▷ Update states
33:    $q_j = Q(v_j^l)$ ;
34: end for
35: return  $q$ 

```

---